Received September 2, 2020, accepted September 20, 2020, date of publication September 24, 2020,
date of current version October 12, 2020.

Digital Object Identifier 10.1109/ACCESS.2020.3026372

Endoscopic Probe for Ultrasound-Assisted Photodynamic Therapy of Deep-Lying Tissue

JINWOO KIM, (Student Member, IEEE), HAEMIN KIM, AND JIN HO CHANG, (Senior Member, IEEE)

Department of Information and Communication Engineering, Daegu Gyeongbuk Institute of Science and Technology, Daegu 42988, South Korea

Corresponding author: Jin Ho Chang (jhchang@dgist.ac.kr)

This work was supported in part by the National Research Foundation of Korea funded by the Ministry of Science and ICT under Grant NRF-2017R1A2B2002838 and Grant NRF-2019R1I1A1A01061963, and in part by the Daegu Gyeongbuk Institute of Science and Technology Start-Up Fund Program of the Ministry of Science and ICT under Grant 2020030086.

ABSTRACT Endoscopic photodynamic therapy (PDT) has attracted much attention as a minimally invasive, minimally toxic treatment. PDT can selectively destroy cancer cells by reactive oxygen generated through chemical reaction of photosensitizers that absorb incident light with a certain wavelength. However, the efficacy of PDT is limited due to shallow light penetration mainly caused by Rayleigh scattering in biological tissue. We previously demonstrated that the air bubbles temporarily induced by ultrasound (US) act as a Mie scattering medium, thus increasing light penetration, called US-assisted light penetration increase. For endoscopic applications of the proposed method, the endoscopic probe for US-assisted PDT should be developed; it should be as small as possible while being able to deliver laser for treatment and provide high acoustic energy for air bubble generation in the laser pathway. Satisfying those requirements is very challenging. In this paper, we report a recently developed endoscopic probe for US-assisted PDT that meets the requirements. The probe consists of two 3 MHz US transducers placed side by side and tilted at an angle of 25° and an optical fiber for laser delivery. The probe size was measured at 60.5 mm × 14 mm × 14 mm suitable for endoscopic applications. In the experiment, it was shown that the probe could increase the laser intensity by 28%, compared to the laser only illumination. Even this increase is higher than the previous measurement using a commercial ring-shaped 1.1 MHz HIFU transducer with outer and inner diameters of 64 mm and 22.6 mm.

INDEX TERMS Ultrasonic transducers, biomedical transducers, biophotonics, light scattering, photodynamic therapy, ultrasound-induced microbubbles.

I. INTRODUCTION

Endoscopy has been used to diagnose diseases by inserting an endoscope through the mouse or the anus and observing the inside of the body [1], [2]. In addition to diagnosis, treatment can be performed with an endoscope, which is called therapeutic endoscopy [3]. Compared to traditional surgery requiring a large incision, therapeutic endoscopy has low complications and mortality related to surgical procedure [4], and it is suitable for simultaneous diagnosis and therapy [5]. For these reasons, therapeutic endoscopy has been in the spotlight as a noninvasive or minimally invasive theragnostic tool, especially, for cancer occurring in the organs of the digestive system such as the gastrointestinal, colon, duodenum, and pancreas, where a therapeutic endoscope is easily accessible; endoscopic mucosal resection (EMR), endoscopic polypectomy, and endoscopic submucosal dissection (ESD) are the typical examples of therapeutic endoscopy [6], [7]. However, these methods have a risk of complications such as perforation and hemorrhage and a high possibility of recurrence due to incomplete incision [4], [7]–[9]. Endoscopic photodynamic therapy (PDT) has attracted much attention as a viable solution to the aforementioned problems of therapeutic endoscopy [10], [11].

PDT rests on photosensitized oxidation reactions in which a photosensitizer absorbing irradiated light produces a highly reactive oxygen species such as singlet oxygen, thus leading to the chemical destruction of cancer cells [12]. For PDT, photosensitizers are administered to accumulate in a tumor site and light is illuminated to the site. Effective PDT can be performed using light with a wavelength at which the photosensitizers have the peak absorbance, thus facilitating the selective destruction of tumor cells with minimal or no damage to normal tissue. Another advantage of PDT is the capability of repeated treatment and the ease of combination with diagnostic methods [12]–[15]. However, these benefits

The associate editor coordinating the review of this manuscript and approving it for publication was Zeev Zalevsky.

are only available if sufficient light energy can reach the target lesion, but optical scattering in biological media open hinders maximizing the benefits of PDT because it limits penetration depth of illuminated light. To make the matter worse, additionally, low light energy is required for safe treatment [16].

The most practical solution to the insufficient penetration depth of light is the development of high performance photosensitizers that have the peak absorbance at a desired wavelength within the near-infrared (NIR) window in the range of 600 to 900 nm and the capability of high selective accumulation in a target lesion [12], [17], [18]. Note that the absorbance of endogenous chromophores is low within the NIR window, so that the energy loss of irradiated light due to light absorption can be minimized. Implantable light sources can be used to reduce the distance that the light travels to the tumor site [19] if a module capable of elaborate insertions is available to avoid tissue perforation. As another approach, we proposed a way to mitigate the adverse effect of optical scattering itself on the penetration depth of light [20]. This method is based on the fact that ultrasound (US) can temporarily generate air bubbles in the light path and the bubbles act as a Mie scattering medium. Note that Rayleigh scattering, the main cause of the limited penetration depth of light, occurs in all directions, whereas Mie scattering arises primarily in the forward direction equal to light propagating direction. Therefore, the US-induced air bubbles result in increasing the penetration depth of light and alleviating the defocusing of light.

This US-assisted light penetration increase can be used for optical imaging and therapy. For this, new US transducers capable of generating acoustic energy high enough to induce air bubbles should be developed to suit specific applications. Since the aperture size of a transducer is linearly proportional to the strength of generated acoustic energy [21], it is very challenging to develop a transducer that has the capability to produce high acoustic energy for US-assisted endoscopic PDT. This is so because the maximum diameter of an endoscopic probe was reported to be 14.6 mm [22], and both optical module and US transducer should be integrated into an US-assisted endoscopic probe. This means that an increase in transducer aperture is limited and it is difficult to deliver enough US energy for generating air bubbles in tissue. In this paper, we report a recently developed endoscopic probe for US-assisted PDT. The design and fabrication of the compact endoscopic PDT probe are described, and it is demonstrated that the developed probe is able to generate air bubbles and increase the intensity of light irradiated simultaneously with the US energy due to lowering optical scattering and defocusing.

II. ENDOSCOPIC PROBE FOR US-ASSISTED PDT

A. CONCEPT AND DESIGN

For conventional endoscopic PDT, light is illuminated to a tumor after injecting photosensitizers, and it experiences Rayleigh scattering in tissue before reaching the tumor as shown in Fig. 1(a). This scattering causes the energy loss and defocusing of the irradiated light. Due to this, the optimum depth of PDT is up to 10 mm [23], [24], and it is difficult to treat tumors larger than 10 mm in diameter [25]. The US-assisted endoscopic PDT is performed by transmitting US and light simultaneously as shown in Fig. 1(b). In the light pathway, the US energy induces air bubbles that serve as a Mie scattering medium. Considering the fact that air bubbles are generated at a focal depth of US towards a transducer [26] as well as the location and size of tumors occurring in the digestive system, the focal length of the endoscopic probe for US-assisted PDT was determined to be over 10 mm. Since it is difficult to achieve an F-number of unity by physical conformation or acoustic lens [21], the size of the transducer aperture should be less than 10 mm in diameter, considering the desired focal length, i.e., over 10 mm. Note that the F-number is defined as the ratio of focal length to aperture diameter. For light delivery, an optical fiber with a diameter of 600 μm was selected. The full width at half maximum (FWHM) of the light delivered through the optical fiber was determined to be 2 mm.

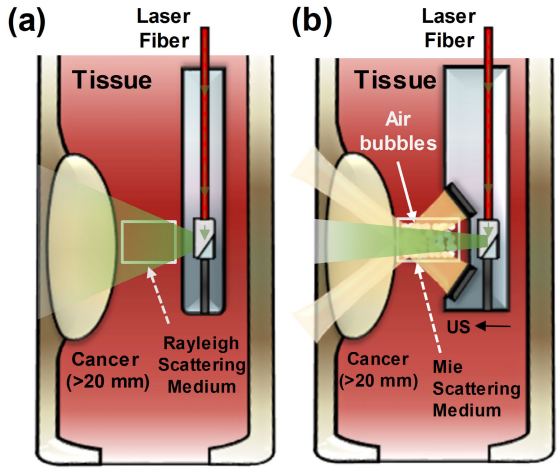

FIGURE 1. Conceptual illustration of endoscopic PDT: (a) conventional PDT and (b) proposed ultrasound (US)-assisted PDT. Optical scattering occurs in the all directions in the case of Rayleigh scattering media, whereas Mie scattering arises primarily in the forward direction. The air bubbles (indicated by yellow circles in (b)) temporarily generated by US serves as a Mie scattering medium, thus resulting in increased penetration depth of light and therapeutic depth.

Since air bubbles need to be generated in the path of light propagation, the focal area of an US transducer should lie on the path. The direct approach to this is to create an opening in the center of a transducer, which allows light to be illuminated through the opening and propagated along the US beam axis called the axial axis in US imaging [27]. However, this direct method is difficult to use for a compact transducer due to not only fabrication difficulties but also acoustic energy loss. For example, an US energy loss of 16% occurs when a hole with a diameter of 4 mm is created in a transducer aperture of 10 mm in diameter. This energy loss may be critical because it is even challenging to achieve acoustic intensity high enough to generate a bubble cloud using a transducer with an aperture

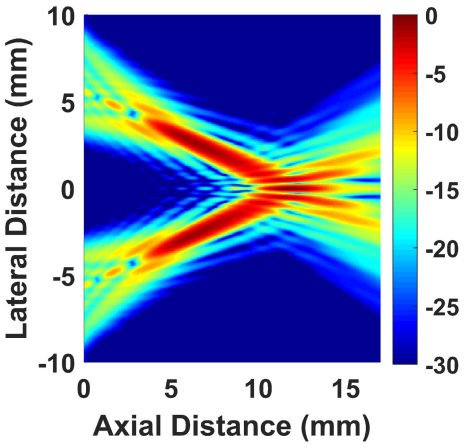

FIGURE 2. Beam profile simulated using a Field II program when the two US transducers with a center frequency of 3 MHz and a tilt angle of 25° were used to transmit US waves.

diameter of 10 mm. Therefore, we chose to use two US transducers placed side by side and tilted at a certain angle as shown in Fig. 1(b). The tilt angle was determined to overlap two beam profiles generated by the two transducers in the desired region where air bubbles are produced.

Beam simulation was performed to select the tilt angle and center frequency of the US transducers using a Field II program [28] because the two parameters mainly determine the effective area in which air bubbles are generated. Since we used light with a beam width of 2 mm in diameter, the size of a bubble cloud should be larger than 2 mm in the lateral direction perpendicular to the axial direction (i.e., both US and light propagation direction). It was assumed that a bubble cloud occurs in the region of normalized US beam intensity higher than −10 dB. In the simulation, the transducer with a size of 7.2 mm in diameter and a focal length of 12 mm was used, which met the requirements for the aperture size and focal length of the transducer. The gap between the two transducers was determined to be 7 mm, considering easy fabrication. Given the parameters selected above, the center frequency and tilt angle were found to meet the requirements for the intensity. For this, the simulation was conducted by changing the center frequency of the transducer from 1 to 3 MHz at 1 MHz intervals and the title angle from 15 to 35° at 5° intervals. Based on the simulation results, we selected a center frequency of 3 MHz and a title angle of 25°. The maximum intensity of the beam generated by the two transducers was located at a depth of 10.7 mm, the −6 dB and −10 dB lateral beam widths were 1.30 and 2.2 mm, respectively. Also, the −6 dB and −10 dB depth of focuses (DOFs) were measured at 3.5 and 4.65 mm (see Fig. 2).

B. FABRICATION AND INTEGRATION

Strontium-modified lead zirconate titanate (PZT-4) was selected for producing US energy high enough to induce air bubbles; PZT-4 is a popular piezoelectric material used for a high-intensity focused ultrasound (HIFU) transducer because of its high transmission efficiency [29], [30].

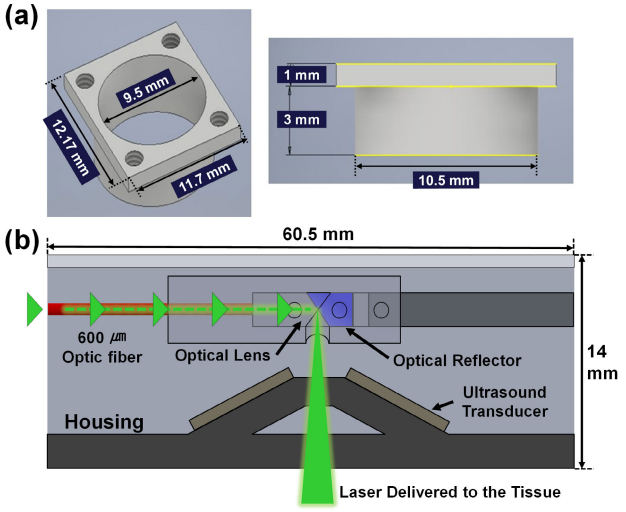

FIGURE 3. (a) Schematic of the brass housing and (b) conceptual illustration of the developed endoscopic probe for ultrasound-assisted photodynamic therapy.

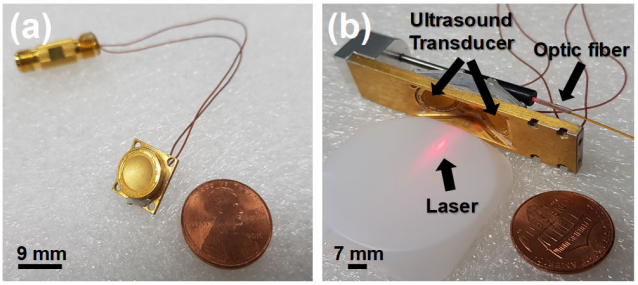

FIGURE 4. Photographs of (a) the developed single element transducer and (b) inside the finished endoscopic probe with integrated the two single element transducers and the optical module.

Two custom-made circular PZT-4 materials with a focal length of 12 mm and a diameter of 7.2 mm (Dong Il Technology LTD., Gyeonggi-do, South Korea) were prepared. No acoustic matching layers were used for a narrow spectral bandwidth, and air backing was employed for achieving the maximum transmitted acoustic power. A brass housing was constructed, as shown in Fig. 3(a); it had a well with inner and outer diameters of 9.5 and 10.5 mm, a height of 3 mm, and the square bottom with a size of 12.17 mm × 11.7 mm × 1 mm. One circular PZT-4 material was fixed to the glass plate by using 5-min Epoxy (ITW Polymers Adhesives North America, Danvers, MA, USA), and the well in the housing was laid down on the plate. Epo-tek 314 (Epoxy technologies, Billerica, MA, USA) was poured into the well for electrical shielding and heated to 120°C for 3 hours. After cooled down at room temperature, the front of the brass housing was sputtered with Cr/Au (1000/4000Å) for ground connection between the housing and the PZT-4. One ground and one signal wires were connected to the front of the housing and the backside of the PZT-4, which were connected to a SMA (Subminiature version A) connector (see Fig. 4(a)).

The housing of the endoscopic probe for US-assisted PDT was designed and constructed (Fig. 3(b)); the size was 60.5 mm × 14 mm × 14 mm suitable for

endoscopic applications. The housing is designed to have a structure that can be easily assembled using screws. Therefore, the sophisticated design of the housing can reduce the overall dimension considerably. The housing contained a support for placing the two transducers at a tilt angle of 25°. The support had two square holes to fix the two transducers and one circular hole with a diameter of 2 mm to deliver laser. After placing the two transducers in the square holes, Cr/Au (1000/4000Å) sputtering was performed again to connect two electrical grounds. For laser delivery, an optical fiber with a diameter of 600 μm (SM600, Thorlabs Inc., Newton, New Jersey, USA) was used, and an optical lens (LightPath 354430, Edmund Optics, Barrington, New Jersey, USA) and an optical reflector (TECHSPEC 45° Rod Mirror, Edmund Optics, Barrington, New Jersey, USA) were placed in front of an optical fiber to allow laser to illuminate the treatment area and ensure the desired beam size in the area. Figure 4(b) shows the inside of the developed endoscopic probe for US-assisted PDT.

III. CHARACTERISTICS AND PERFORMANCE EVALUATION

A. CHARACTERISTICS

The pulse-echo test was performed to assess the center frequency and −6 dB fractional bandwidth of the developed single element transducer (Fig. 4(a)). For this, a stainless-steel target was place on the bottom of a container filled with deionized, degassed water. The transducer was immersed into the container, and the distance between the target and the transducer was adjusted to place the target at the focal point of the transducer. A pulser/receiver system with an output electrical impedance of 50 Ω (5800PR, Olympus, Japan) was used to excite the transducer with an energy of 12.5 μJ and receive the echo from the target. A digital oscilloscope (TDS7054, Tektronix Inc., Beaverton, OR, USA) was used to digitize and record the echo signals. As shown in Fig. 5, the center frequency and −6 dB fractional bandwidth of the single element transducer were measured at 3.095 MHz and 0.436 MHz, respectively.

The electrical impedance of the transducer was measured to determine the optimal electrical signal frequency used for exciting both transducers simultaneously. The measurement was performed in the frequency range from 1 to 7 MHz at 0.05 MHz intervals by using an impedance analyzer with z-probe attachment (HP4294A, Agilent Technologies Inc., Santa Clara, CA, USA). It should be noted that the two signal wires were connected to each other for the all experiments including the electrical impedance and beam profile measurements because the electrical impedance of the probe should be reduced, as will be discussed later. In addition, the signal connection allowed for using one function generator (AFG3102C, Tektronix Inc., Beaverton, OR, USA) to excite the two transducers at the same time in performance evaluation. As shown in Fig. 6, the developed probe had the electrical impedance with a resonance frequency of 2.96 MHz and an anti-resonance frequency of 3.31 MHz. The magnitude

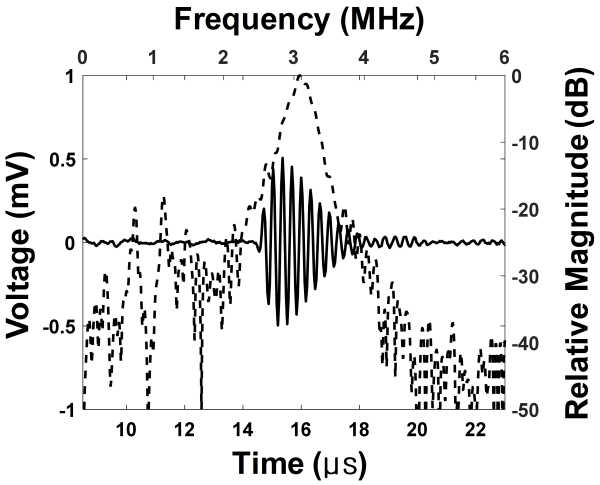

FIGURE 5. Pulse-echo response of the developed single element transducer (solid line) and its frequency spectrum (dashed line).

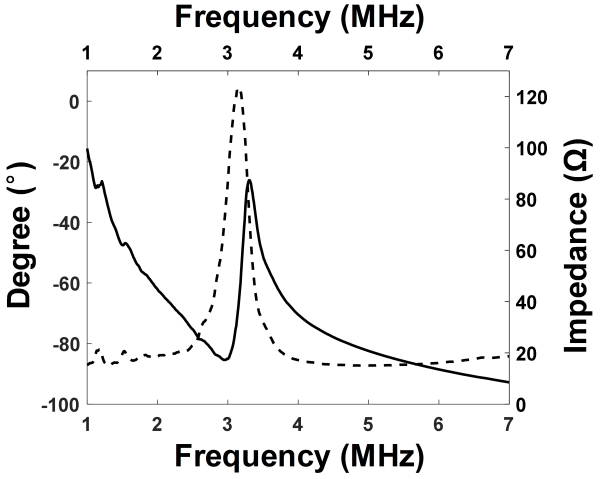

FIGURE 6. Measured electrical impedance of the developed single element transducer. The solid and dotted lines indicate the magnitude and phase angle of the electrical impedance, respectively.

and phase angle of the electrical impedance at the resonance frequency were 17.24 Ω and −37.44°, and those at the anti-resonance were 87.33 Ω and −39.79°. The center between the resonance and anti-resonance frequencies were 3.14 MHz at which the magnitude and phase angle were 35.71 Ω and 3.29°. Based on the experimental results, we decided to find the optimal frequency of the electrical signal for exciting the transducers in the range of 2.6 to 3.6 MHz, so that the endoscopic probe could produce the maximum US intensity.

The beam profile of the developed endoscopic probe was measured using the AIMS (Acoustic Intensity Measurement System, ONDA Corporation, Sunnyvale, CA, USA) equipped with a needle hydrophone (HGL-0085) to find the focal length of the probe and the optimum frequency at which the probe could generate the maximum US intensity. For the measurement, the endoscopic probe was aligned horizontally to the hydrophone, which was conducted using a motorized two-rotational axis. After find the focal length, the tone-burst

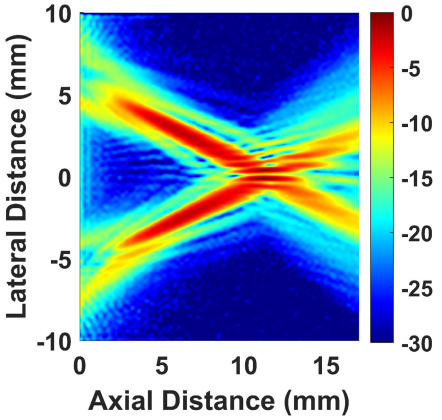

FIGURE 7. Measured Beam profile after the two US transducers with a center frequency of 3 MHz and a tilt angle of 25° were excited at the same time.

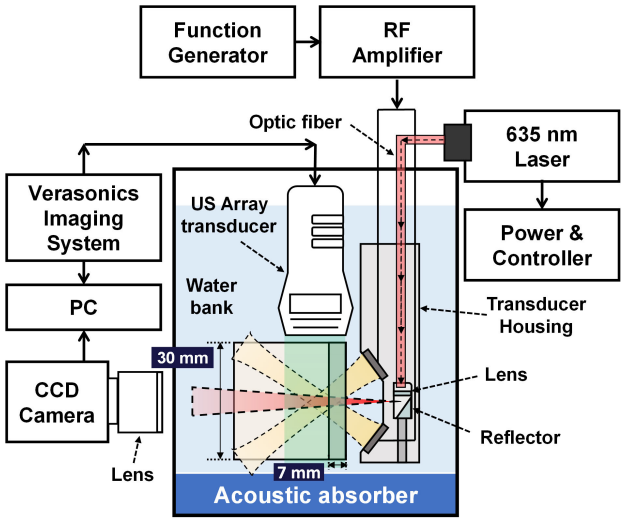

FIGURE 8. Experimental Arrangement for performance evaluation of developed endoscopic probe for US-assisted PDT: ability to generate air bubbles and to increase light penetration.

electrical signal was produced by the function generator and applied to the probe. For each measurement, the frequency of the tone-burst electrical signal was changed from 2.6 to 3.6 MHz at 0.05 MHz intervals to determine the optimal frequency at which the maximum US intensity occurred at the focus. The electrical signal had 10 V peak-to-peak voltage, 10 cycles, and 1 ms pulse repetition period. The focal length of the probe was measured at 11.23 mm, and the maximum US intensity was obtained when the electrical signal frequency was 3.15 MHz. In this case, the measured beam profile after applying the 3.15 MHz electrical signal to the probe had −6 dB and −10 dB lateral beam widths of 1.26 and 2.27 mm at the focal point (see Fig. 7); the −6 dB and −10 dB DOFs were 3.19 and 3.96 mm, which were in good agreement with the Field II simulation results. In addition, it was found that the acoustic pressure could increase by 25% when the two transducers generated US simultaneously, compared to one transducer.

B. PERFORMANCE EVALUATION

The performances of the developed endoscopic probe for US-assisted PDT were evaluated in two aspects: abilities to generate air bubbles in the desired area and to increase light intensity. The evaluation was conducted through phantom experiments. For this, tissue-mimicking phantoms were constructed, which had three sections; the front and rear sections were non-scattering media, and the middle section was a scattering medium. The 18-mm thick rear section (i.e., non-scattering medium) was made using acrylamide-bovine serum albumin (BSA) mixture; the recipe for the mixture can be found in [31]. For the middle section, an intralipid-20% of 1% (v/v) as optical scatterers was mixed with the acrylamide-BSA mixture, which was poured onto the rear section and hardened at room temperature. Rayleigh scattering and air bubble generation occurred in the middle section of which thickness was 7 mm. Finally, the 5-mm thin front section was constructed on the middle section. Note that the laser used for this study was unable to penetrate the 12-mm thick scattering section at all when air bubbles were not generated. To demonstrate that the air bubbles can reduce scattering and defocusing by comparing laser energy distributions, we used the non-scattering front section. For the performance evaluation, the phantom was placed on the bottom of a container filled with degassed water, as shown in Fig. 8.

The developed endoscopic probe was placed on the front section of the phantom to generate air bubbles in the middle section. For this experiment, tone-burst electrical signals with 97 $V_{p\text{-}p}$, 52,500 cycles, and 50 ms pulse repetition period were generated using the function generator and a radio-frequency power amplifier with a gain of 55 dB (75A250A, Amplifier Research Corp., Souderton, PA, USA). In this case, the I_{SPTP} (spatial-peak temporal-peak intensity) of the US generated by the probe was estimated to be 174 W/cm^2. Note that the tone-burst signal had a center frequency of 3.15 MHz because it was experimentally found that the probe could produce the maximum peak pressure at the focal depth when it was excited with 3.15 MHz electrical signals. Air bubble generation was observed using a commercial US imaging system (Vantage Research Ultrasound System, Verasonics Inc., Kirkland, WA, USA) equipped with an US imaging transducer (L7-4, Verasonics Inc.). The imaging probe was positioned on the side of the phantom for visualization of the generated air bubbles (see Fig. 8).

As shown in Fig. 9, the developed endoscopic probe was able to generate air bubbles in spite of its small size. Note that air bubbles appear bright in US images because these are a hyperechogenic medium [27]. The bubble cloud had a lateral width of 3.15 mm at the focal point and an axial length of 5.90 mm. The size was consistent with the measured size of the −13 dB level of the beam profile shown in Fig. 7. Especially, the lateral size of the bubble cloud was large enough to accommodate the incident laser beam with a diameter of 2 mm used in this study. As a result, the bubble cloud generated by the probe was expected to act as a Mie scattering medium, and thus no (or minimal) laser beam spread would occur due to optical scattering when the cloud existed.

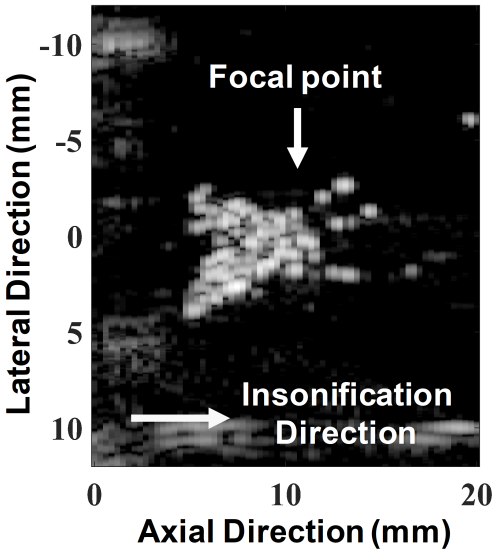

FIGURE 9. Ultrasound image of the air bubble cloud produced by the developed endoscopic probe for US-assisted PDT.

The effect of the generated air bubbles on beam spread was investigated. For this, a continuous wave (CW) laser with a wavelength of 635 nm (MDL-XD-635, CNI Optoelectronics Technology Co. Ltd., Changchun, China) was emitted through the optical fiber while generating the bubble cloud. The laser beam had a Gaussian profile with a FWHM of 2 mm. The laser power was 265 mW. The light intensity was measured using a charge-coupled device (CCD) camera (CoolSNAP MYO, Photometrics, Tucson, AZ, USA) that was placed behind the phantom (see Fig. 8); the distance from the phantom was 15 cm. An optical lens (Micro-Nikkor 105 mm f/2.8, Nikon Corp., Tokyo, and Japan) was positioned between the CCD camera and the phantom to measure the light intensity at the end of the middle section. In the measurement, the exposure time of the camera was 300 ms.

As expected, the light intensity distribution obtained after solely delivering the laser into the phantom showed that both defocusing and scattering occurred in the phantom severely, as shown in Fig. 10(a). The light intensity distribution exhibited severe fluctuation along the horizontal axis of Fig. 10(b), due to optical scattering. Additionally, it was observed that defocusing occurred; the FWHM broadened from 2 mm to 2.63 mm. In contrast, both scattering and defocusing were slackened when the laser was irradiated after the air bubbles were generated in the scattering medium by using US with an I_{SPTP} of 174 W/cm^2 (see Fig. 10(c)). The light intensity distribution was restored to the Gaussian shape, as shown in Fig. 10(d). The FWHM was measured at 2.05 mm, which was similar to that of the laser before entering the phantom. In addition, the light intensity produced by the US-assisted laser delivery was increased by 28%, compared to the laser only illumination; this means that the developed probe can increase light penetration depth under the same conditions of laser intensity.

To predict the benefit of the developed endoscopic probe for PDT, fluorescence, produced in fluorescent dyes (Alexa Fluor 660, Thermo Fisher Scientific Inc., Waltham, MA, USA) after absorbing light, was measured. A 2-mm diameter hole was created in the surface of the rear section of the phantom, and the dyes were injected in the hole. After covering the hole with the light scattering medium with a thickness of 7 mm, the phantom was immersed into the water container. When solely transmitting US with an I_{SPTP} of 153.8 W/cm^2, no florescence was measured, as shown in Fig. 11(a). This is reasonable because the dyes do not react to US energy. When the laser with a power of 265 mW was solely delivered to the phantom, the average intensity of measured fluorescence was 629 a.u. (see Fig. 11(b)). The intensity increased by about 50% when delivering both laser and US at the same time (see Fig. 11(c)). Consequently, the results demonstrated that the compact endoscopic probe developed for US-assisted PDT is able to generate air bubbles in the desired scattering medium, reduce optical scattering, and increase laser intensity, although the size of the probe is small enough for endoscopic applications.

IV. DISCUSSION

For efficient US-assisted PDT, the size and position of the bubble cloud created by the endoscopic probe should be controllable. As shown in [20], the bubble cloud grows mainly in the axial direction as US intensity increases. Additionally, the cloud growth direction is towards an US transducer [26], which is also confirmed in Fig. 9. This is so because air bubbles are generally considered to be high US reflecting media. As a result, a focal length of 10.7 mm, formed by the two US transducers, is the maximum depth of a bubble cloud and reasonable for tumor size and occurrence location. Note that the optimum treatment depth of the conventional PDT is up to 10 mm [23], [24]. Therefore, superficial tumors can also be treated with the developed endoscopic probe by emitting only laser without the air bubble generation; in this case, the two US transducers may be used simultaneously for thermal ablation of the tumors.

One the other hand, the cloud size in the lateral direction is less adjustable. As shown in Fig. 9, the bubble cloud was cross-shaped because the cloud growth occurred along the paths of the two US beams generated by the two transducers (see Fig. 7). Therefore, the narrowest width of the cloud in the lateral direction was exhibited at the focal point. Due to the US beam shape, the developed probe may be less efficient for completely filling the air bubbles in the laser pathway although the lateral size of the cloud is large enough to cover the laser. To this end, a single element transducer with a small opening in the center needs to be developed in order to take full advantage of US-assisted PDT although it is demanding. Another possible solution is to fabricate a single element transducer using optically transparent acoustic modules [32]; the epoxy used for the transparent transducer for photoacoustic microscopy may not be the best material for acoustic lens for air bubble generation because of its

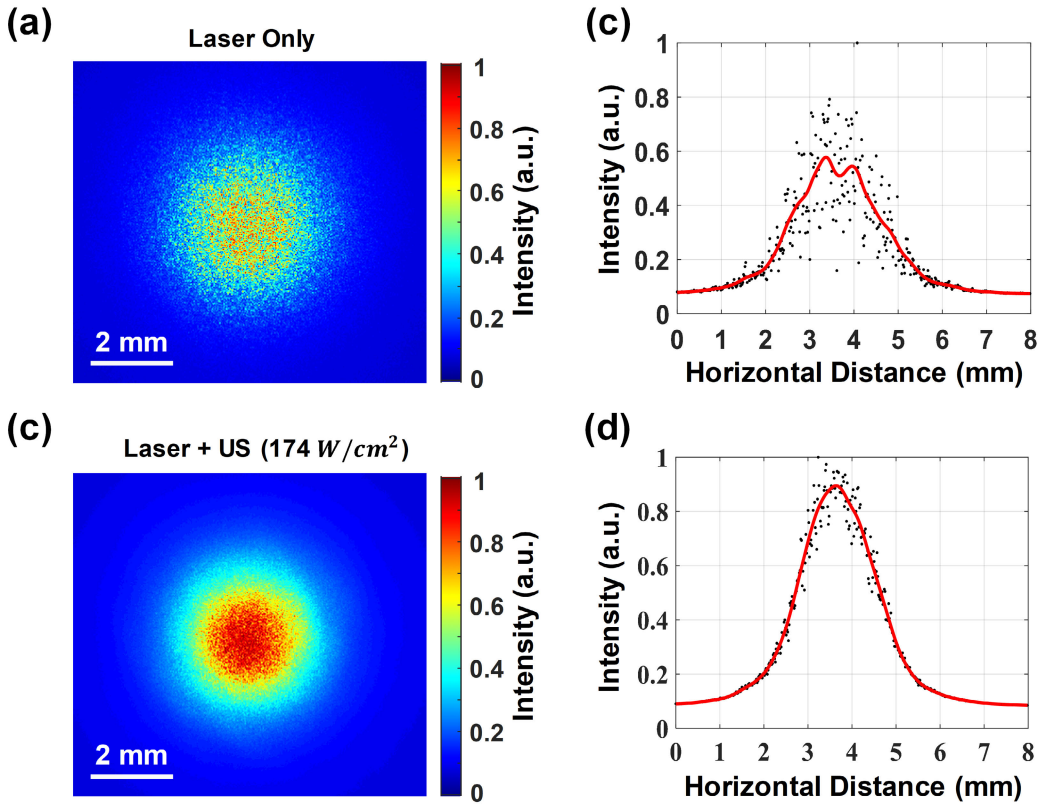

FIGURE 10. (a) Light intensity distribution measured at the end of the phantom after only the laser was irradiated. (b) Distribution along the horizontal axis of (a) (black dots) and the corresponding smoothing spine curve fitting (red line). (c) Light intensity distribution measured after both laser and ultrasound (US) with an intensity of 174 W/cm^2 was irradiated and (d) corresponding distribution along the horizontal axis of (c).

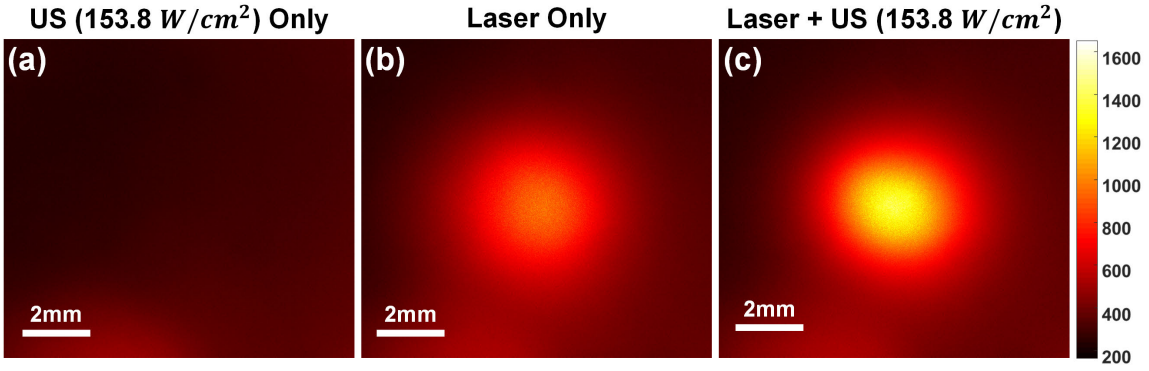

FIGURE 11. Fluorescence intensity distribution measured after (a) only US with an intensity of 153.8 W/cm^2, (b) only laser with a power of 265 mW, and (c) both laser and US were transmitted to the fluorescent dye-contained hole created in the tissue mimicking phantom.

relatively high US attenuation. Therefore, there is a need to develop new acoustic lens materials with low ultrasound attenuation as well as optical transparency.

It is important that the electrical impedance of an US transducer is well matched with an electrical signal generator in view of the efficient transmission of electrical power to the transducer [33]. This is particularly true for HIFU applications including the bubble generation [34]. Since an US transducer can be considered as a capacitive device [35], the electrical impedance of an US transducer is proportional to the thickness of a piezoelectric material and inversely proportional to its area. Note that the thickness is also inversely proportional to the center frequency of an US transducer. For US-assisted endoscopic PDT, the size of the US transducer should be as small as possible while still being able to provide high acoustic energy enough for bubble generation. To this end, each transducer in the developed endoscopic probe inevitably had a relatively high electrical impedance, as summarized in Table 1. Note that general electrical signal generators used for exciting a transducer have low output impedance (i.e., 5–10 Ω) [36]. For efficient bubble generation, therefore, the two US transducers were

TABLE 1. Measured electrical impedance of right, left, and parallel connected transducers in the developed probe.

Right Element	Resonance Frequency (3.01 MHz)	Anti-resonance Frequency (3.32 MHZ)	Center Frequency (3.17 MHZ)
Magnitude (Ω)	37.88	179.3	85.88
Phase (°)	–34.57	–41.3	2.37
Left Element	**Resonance Frequency (2.96 MHz)**	**Anti-resonance Frequency (3.31 MHZ)**	**Center Frequency (3.14 MHZ)**
Magnitude (Ω)	38.54	155.5	72.89
Phase (°)	–41.8	–44.63	–8.45
Parallel Connection	**Resonance Frequency (2.96 MHz)**	**Anti-resonance Frequency (3.31 MHZ)**	**Center Frequency (3.14 MHZ)**
Magnitude (Ω)	17.24	87.33	35.71
Phase (°)	–37.44	–39.79	3.29

connected in parallel; two signal wires and two ground wires were connected to each other, respectively. By doing so, the electrical impedance of the probe was reduced by about half, i.e., from 85.88 Ω and 72.89 Ω to 35.71 Ω.

The threshold for bubble generation is mainly determined by a negative pressure induced by an US transducer, and the size of bubble cloud depends on pulse duration, operating frequency, and duty cycle [37]. Additionally, the threshold increases as US frequency increases [38]. From this point of view, a center frequency of 3 MHz employed for the developed probe may not be efficient for bubble generation. However, the electrical impedance of a transducer, which is the same size as the developed transducer and whose center frequency is 1 MHz or less, can be estimated to be several hundred ohms. This is because the electrical impedance increases as the center frequency and area of a transducer decrease. The high electrical impedance makes it difficult to perform electrical impedance matching to an electrical signal generator in an externally located system. This degree of electrical impedance mismatching hinders the maximum electrical power transmission to the transducer. Note that conventional HIFU transducers have a center frequency of 1 MHz or less. On the other hand, high frequency is more beneficial for accurate targeting of treatment region and no thermal damage to the tissue in the laser pathway [35], [39].

V. CONCLUSION

An endoscopic probe for US-assisted PDT should be able to provide high acoustic energy to generate air bubbles in the laser path and deliver laser for treatment simultaneously. In addition, its size should be as small as possible. Satisfying those requirements is very challenging. In this paper, we showed that the developed probe, in which the two US transducers were placed side by side and tilted at an angle of 25°, had the ability to generate a bubble cloud in the laser pathway, reduce optical scattering, and increase laser intensity despite its small size suitable for endoscopic applications: 60.5 mm × 14 mm × 14 mm. In the experiment, it was shown that the probe could increase the laser intensity by 28%, compared to the laser only illumination. Even this increase is higher than the previous measurement using a commercial ring-shaped HIFU transducer with outer and inner diameters of 64 mm and 22.6 mm, and a center frequency of 1.1 MHz [20]. As a result, we believe that the development of the endoscopic probe for US-assisted PDT can open up another way to overcome the limitations of conventional PDT although its treatment efficacy should be evaluated in vivo.

REFERENCES

[1] J. East, J. Vleugels, P. Roelandt, P. Bhandari, R. Bisschops, E. Dekker, C. Hassan, G. Horgan, R. Kiesslich, G. Longcroft-Wheaton, A. Wilson, and J.-M. Dumonceau, "Advanced endoscopic imaging: European society of gastrointestinal endoscopy (ESGE) technology review," *Endoscopy*, vol. 48, no. 11, pp. 1029–1045, Oct. 2016.
[2] I. C. Roberts-Thomson, R. Singh, E. Teo, N. Q. Nguyen, and I. Lidums, "The future of endoscopy," *J. Gastroenterol. Hepatol.*, vol. 25, no. 6, pp. 1051–1057, Jun. 2010.
[3] P. J. Pasricha, "The future of therapeutic endoscopy," *Clin. Gastroenterol. Hepatol.*, vol. 2, no. 4, pp. 286–289, Apr. 2004.
[4] F. A. C. Bustamante, E. G. Hourneaux DE Moura, W. Bernardo, R. A. A. Sallum, E. Ide, and E. Baba, "Surgery versus endoscopic therapies for early cancer and high-grade dysplasia in the esophagus: A systematic review," *Arquivos de Gastroenterologia*, vol. 53, no. 1, pp. 9–10, Mar. 2016.
[5] E. J. Kuipers and J. Haringsma, "Diagnostic and therapeutic endoscopy," *J. Surg. Oncol.*, vol. 92, no. 3, pp. 203–209, Dec. 2005.
[6] D. Weinberg, S. Heller, and J. Tokar, "Current status of advanced gastrointestinal endoscopy training fellowships in the United States," *Adv. Med. Educ. Pract.*, vol. 2, p. 25, Jan. 2011.
[7] P. C. De Groen, "History of the endoscope [scanning our past]," *Proc. IEEE*, vol. 105, no. 10, pp. 1987–1995, Oct. 2017.
[8] M. O. Othman and M. B. Wallace, "Endoscopic mucosal resection (EMR) and endoscopic submucosal dissection (ESD) in 2011, a Western perspective," *Clinics Res. Hepatol. Gastroenterol.*, vol. 35, no. 4, pp. 288–294, Apr. 2011.
[9] A. Mao, "Interventional therapy of esophageal cancer," *Gastrointestinal Tumors*, vol. 3, no. 2, pp. 59–68, Oct. 2016.
[10] H. H. Lee, M.-G. Choi, and T. Hasan, "Application of photodynamic therapy in gastrointestinal disorders: An outdated or re-emerging technique?" *Korean J. Internal Med.*, vol. 32, no. 1, pp. 1–10, Jan. 2017.
[11] H. Wu, T. Minamide, and T. Yano, "Role of photodynamic therapy in the treatment of esophageal cancer," *Digestive Endoscopy*, vol. 31, no. 5, pp. 508–516, Sep. 2019.
[12] I. Yoon, J. Z. Li, and Y. K. Shim, "Advance in photosensitizers and light delivery for photodynamic therapy," *Clin. Endoscopy*, vol. 46, no. 1, p. 7, Jan. 2013.
[13] Á. Juarranz, P. Jaén, F. Sanz-Rodríguez, J. Cuevas, and S. González, "Photodynamic therapy of cancer. Basic principles and applications," *Clin. Transl. Oncol.*, vol. 10, no. 3, pp. 148–154, Mar. 2008.
[14] H.-H. Chan, N. S. Nishioka, M. Mino, G. Y. Lauwers, W. P. Puricelli, K. N. Collier, and W. R. Brugge, "EUS-guided photodynamic therapy of the pancreas: A pilot study," *Gastrointestinal Endoscopy*, vol. 59, no. 1, pp. 95–99, Jan. 2004.
[15] N. Muhanna, L. Cui, H. Chan, L. Burgess, C. S. Jin, T. D. MacDonald, E. Huynh, F. Wang, J. Chen, J. C. Irish, and G. Zheng, "Multimodal image-guided surgical and photodynamic interventions in head and neck cancer: From primary tumor to metastatic drainage," *Clin. Cancer Res.*, vol. 22, no. 4, pp. 961–970, Feb. 2016.
[16] F. Borgia, R. Giuffrida, E. Caradonna, M. Vaccaro, F. Guarneri, and S. Cannavò, "Early and late onset side effects of photodynamic therapy," *Biomedicines*, vol. 6, no. 1, p. 12, Jan. 2018.
[17] B. C. Wilson, "Photodynamic therapy for cancer: Principles," *Can. J. Gastroenterol.*, vol. 16, no. 6, pp. 393–396, Jul. 2002.

[18] S. Mallidi, S. Anbil, A.-L. Bulin, G. Obaid, M. Ichikawa, and T. Hasan, "Beyond the barriers of light penetration: Strategies, perspectives and possibilities for photodynamic therapy," *Theranostics*, vol. 6, no. 13, pp. 2458–2487, Oct. 2016.
[19] A. Kim, J. Zhou, S. Samaddar, S. H. Song, B. D. Elzey, D. H. Thompson, and B. Ziaie, "An implantable ultrasonically-powered micro-light-source (μLight) for photodynamic therapy," *Sci. Rep.*, vol. 9, no. 1, p. 1395, Dec. 2019.
[20] H. Kim and J. H. Chang, "Increased light penetration due to ultrasound-induced air bubbles in optical scattering media," *Sci. Rep.*, vol. 7, no. 1, p. 16105, Dec. 2017.
[21] J. Jang and J. Chang, "Design and fabrication of double-focused ultrasound transducers to achieve tight focusing," *Sensors*, vol. 16, no. 8, p. 1248, Aug. 2016.
[22] F. M. Murad, S. Komanduri, B. K. A. Dayyeh, S. S. Chauhan, B. K. Enestvedt, L. L. Fujii-Lau, V. Konda, J. T. Maple, R. Pannala, N. C. Thosani, and S. Banerjee, "Echoendoscopes," *Gastrointestinal Endoscopy*, vol. 82, no. 2, pp. 189–202, Aug. 2015.
[23] H.-B. Ris, H. Altermatt, R. Inderbitzi, R. Hess, B. Nachbur, J. Stewart, Q. Wang, C. Lim, R. Bonnett, and M. Berenbaum, "Photodynamic therapy with chlorins for diffuse malignant mesothelioma: Initial clinical results," *Brit. J. Cancer*, vol. 64, no. 6, pp. 1116–1120, Dec. 1991.
[24] M. Triesscheijn, P. Baas, J. H. M. Schellens, and F. A. Stewart, "Photodynamic therapy in oncology," *Oncologist*, vol. 11, no. 9, pp. 1034–1044, Oct. 2006.
[25] J.-E. Chang, Y. Liu, T. Lee, W. Lee, I. Yoon, and K. Kim, "Tumor size-dependent anticancer efficacy of chlorin derivatives for photodynamic therapy," *Int. J. Mol. Sci.*, vol. 19, no. 6, p. 1596, May 2018.
[26] J. McLaughlan, I. Rivens, T. Leighton, and G. ter Haar, "A study of bubble activity generated in *ex vivo* tissue by high intensity focused ultrasound," *Ultrasound Med. Biol.*, vol. 36, no. 8, pp. 1327–1344, Aug. 2010.
[27] E.-J. Shin, B. Kang, and J. Chang, "Real-time HIFU treatment monitoring using pulse inversion ultrasonic imaging," *Appl. Sci.*, vol. 8, no. 11, p. 2219, Nov. 2018.
[28] J. A. Jensen and N. B. Svendsen, "Calculation of pressure fields from arbitrarily shaped, apodized, and excited ultrasound transducers," *IEEE Trans. Ultrason., Ferroelectr., Freq. Control*, vol. 39, no. 2, pp. 262–267, Mar. 1992.
[29] S. Zhang, R. Xia, L. Lebrun, D. Anderson, and T. R. Shrout, "Piezoelectric materials for high power, high temperature applications," *Mater. Lett.*, vol. 59, no. 27, pp. 3471–3475, Nov. 2005.
[30] J. Jeong, J. Chang, and K. Shung, "Ultrasound transducer and system for real-time simultaneous therapy and diagnosis for noninvasive surgery of prostate tissue," *IEEE Trans. Ultrason., Ferroelectr., Freq. Control*, vol. 56, no. 9, pp. 1913–1922, Sep. 2009.
[31] H. Kim, G. Jo, and J. H. Chang, "Ultrasound-assisted photothermal therapy and real-time treatment monitoring," *Biomed. Opt. Express*, vol. 9, no. 9, p. 4472, 2018.
[32] S. Park, S. Kang, and J. H. Chang, "Optically transparent focused transducers for combined photoacoustic and ultrasound microscopy," *J. Med. Biol. Eng.*, vol. 40, no. 5, pp. 707–718, Oct. 2020, doi: 10.1007/s40846-020-00536-5.
[33] J.-Y. Moon, J. Lee, and J. H. Chang, "Electrical impedance matching networks based on filter structures for high frequency ultrasound transducers," *Sens. Actuators A, Phys.*, vol. 251, pp. 225–233, Nov. 2016.
[34] J. Song, B. Lucht, and K. Hynynen, "Large improvement of the electrical impedance of imaging and high-intensity focused ultrasound (HIFU) phased arrays using multilayer piezoelectric ceramics coupled in lateral mode," *IEEE Trans. Ultrason., Ferroelectr., Freq. Control*, vol. 59, no. 7, pp. 1584–1595, Jul. 2012.
[35] J. H. Cha, B. Kang, J. Jang, and J. H. Chang, "A 15-MHz 1-3 piezocomposite concave array transducer for ophthalmic imaging," *IEEE Trans. Ultrason., Ferroelectr., Freq. Control*, vol. 62, no. 11, pp. 1994–2004, Nov. 2015, doi: 10.1109/TUFFC.2015.007288.
[36] R. E. McKeighen, "Design guidelines for medical ultrasonic arrays," in *Proc. Med. Imag., Ultrason. Transducer Eng.*, May 1998, pp. 2–18.
[37] M. Hoogenboom, D. Eikelenboom, M. H. den Brok, A. Heerschap, J. J. Fütterer, and G. J. Adema, "Mechanical high-intensity focused ultrasound destruction of soft tissue: Working mechanisms and physiologic effects," *Ultrasound Med. Biol.*, vol. 41, no. 6, pp. 1500–1517, Jun. 2015.
[38] J. B. Fowlkes and C. K. Holland, "Discussion of the mechanical index and other exposure parameters," *J. Ultrasound Med.*, vol. 19, no. 2, pp. 143–148, Feb. 2000.
[39] E. Vlaisavljevich, K.-W. Lin, M. T. Warnez, R. Singh, L. Mancia, A. J. Putnam, E. Johnsen, C. Cain, and Z. Xu, "Effects of tissue stiffness, ultrasound frequency, and pressure on histotripsy-induced cavitation bubble behavior," *Phys. Med. Biol.*, vol. 60, no. 6, pp. 2271–2292, Mar. 2015.

JINWOO KIM (Student Member, IEEE) received the B.S. degree in biomedical engineering from Inje University, Gyeongnam, South Korea, in 2018. He is currently pursuing the Ph.D. degree with the Department of Information and Communication Engineering, Daegu Gyeongbuk Institute of Science and Technology (DGIST), Daegu, South Korea. His research interests include design and fabrication of ultrasound transducers for therapy application and high-frequency ultrasound transducers.

HAEMIN KIM received the B.S. degree in biomedical engineering from Yonsei University, Wonju, South Korea, in 2012, and the Ph.D. degree in biomedical engineering from Sogang University, Seoul, South Korea, in 2019. From 2019 to 2020, she was a Postdoctoral Research Fellow with the Institute of Integrated Biotechnology, Sogang University. She is currently a Postdoctoral Researcher with the Department of Information and Communication Engineering, Daegu Gyeongbuk Institute of Science and Technology (DGIST), Daegu, South Korea. Her research interests include combination technique of ultrasound and optic for therapy and imaging, medical imaging, and photo acoustic imaging with contrast agents.

JIN HO CHANG (Senior Member, IEEE) received the B.S. and M.S. degrees in electronic engineering from Sogang University, Seoul, South Korea, in 2000 and 2002, respectively, and the Ph.D. degree in biomedical engineering from the University of Southern California, Los Angeles, CA, USA, in 2007. From 2002 to 2003, he was with the Digital Media Research Laboratory, LG Electronics Inc., Seoul, as a Research Engineer. He was a Postdoctoral Research Associate with the NIH Resource Center for Medical Ultrasonic Transducer Technology, University of Southern California, for a period of two years. From 2010 to 2020, he was an Assistant Professor, an Associate Professor, and a Full Professor with Sogang University. He is currently a Full Professor with the Department of Information and Communication Engineering, Daegu Gyeongbuk Institute of Science and Technology (DGIST), Daegu, South Korea. He has been serving as an Associate Editor for the IEEE TRANSACTIONS ON ULTRASONICS, FERROELECTRICS, AND FREQUENCY CONTROL since 2014. He has also been serving as a Topic Editor for *Photonics* since 2020. His research interests include photo acoustic imaging and its clinical applications, high-frequency ultrasound imaging systems, therapeutic ultrasound, and biomedical signal processing.